Available online at www.sciencedirect.com
SCIENCE DIRECT
Journal of Photochemistry and Photobiology A: Chemistry 181 (2006) 195–202
Journal of Photochemistry and Photobiology A:Chemistry
www.elsevier.com/locate/jphotochem

Azo dye degradation using Fenton type processes assisted by UV irradiation: A kinetic study

Hrvoje Kusic, Natalija Koprivanac *, Lidija Srsan

Faculty of Chemical Engineering and Technology, University of Zagreb, Marulicev trg 19, Zagreb 10000, Croatia

Received 18 July 2005; received in revised form 17 November 2005; accepted 22 November 2005
Available online 18 January 2006

Abstract

Application of Fenton and photo-Fenton type processes, UV/Fe^{2+}/H_2O_2 and UV/Fe^0/H_2O_2, for dye wastewater treatment was investigated. In the first stage of the study, Fenton type processes were optimized regarding the iron catalyst concentration and the iron catalyst/H_2O_2 ratio. In the next step, Fe^{2+}/H_2O_2 and Fe^0/H_2O_2 at optimal process parameters were combined with UV radiation in order to enhance dye degradation. The destruction of model organic pollutant, azo dye C.I. Acid Orange 7 (AO7), was monitored on the basis of decolorization and mineralization extents, determined by UV–vis and TOC analyses, respectively. All studied processes have shown high efficiency in the bleaching of the studied dye model solution with complete decolorization achieved in all cases. Mineralization extents depended on the type and the dosage of added iron catalysts for Fenton type reaction. The highest mineralization extent was achieved by UV/Fe^0/H_2O_2, 90.09% of TOC removal. A quantum yield of AO7 organic dye, $\Phi = 6.5 \times 10^{-3}$ mol Einstein^{-1}, was determined on the basis of decolorization of AO7 by direct photolysis.

Keywords: Azo dye; UV irradiation; AO7 quantum yield; Fenton type processes; Dye degradation

1. Introduction

Synthetic dyes are present in almost all spheres of our everyday life and their application is continuously growing. Azo type of dyes with –N=N– unit as the chromophore in the molecular structure is the largest group of dyes and represents more than a half of the global dye production [1,2]. Over 15% of overall azo dye production is lost during manufacturing and application processes [3]. Colored wastestreams from azo dye production processes and utilization industries pose a major threat to the surrounding ecosystems due to the documented health hazards caused by toxicity and a potentially carcinogenic nature of such organic pollutants [4]. Therefore, the necessity of effective dye wastewater treatment prior to discharge into the effluent is undoubted. One of the major difficulties in treating this type of colored wastewater is the ineffectiveness of biological processes, which are mostly economically suitable processes in comparison with other treatment options [5]. Azo dyes are known to be largely non-biodegradable in aerobic conditions and can be reduced to more hazardous intermediates in anaerobic conditions [6]. Other common commercial processes, such as coagulation/flocculation and adsorption, do not involve chemical transformations, and therefore generally transfer waste components from one phase to another, thus causing secondary loading of environment [7–9].

An attractive, sludge free alternative for the treatment of wide range of organic pollutants present in wastewater, including synthetic dyes, are so called Advanced Oxidation Processes (AOPs). Hydroxyl radicals ($OH^\bullet$), highly reactive species generated in sufficient quantities by AOPs, have the ability to oxidize the majority of the organics present in the wastewater effluents [10]. Common AOPs involve Fenton and Fenton like processes, ozonation, electrochemical oxidation, photolysis with H_2O_2 and O_3, high voltage electrical discharge (corona) process, TiO_2 photocatalysis, radiolysis, water solutions treatment by electronic beams or γ-beams and various combinations of these methods [11,12].

Fenton type processes have shown high efficiency for handling different types of colored wastewater, especially for bleaching [13–15]. Generally, Fenton process involves application of iron salts and hydrogen peroxide to produce hydroxyl radicals, Eqs. (1) and (2) [16]:

$$Fe^{2+} + H_2O_2 \rightarrow Fe^{3+} + OH^- + {}^\bullet OH \quad (1)$$

* Corresponding author. Tel.: +385 1 4597 124; fax: +385 1 4597 143.
E-mail address: nkopri@marie.fkit.hr (N. Koprivanac).

1010-6030/$ – see front matter © 2005 Elsevier B.V. All rights reserved.
doi:10.1016/j.jphotochem.2005.11.024

$$Fe^{3+} + H_2O_2 \rightarrow Fe^{2+} + HO_2^{\bullet} + H^+ \quad (2)$$

Besides OH radical, ferryl ion, FeO^{2+}, as an alternate oxidant could also be considered [16]. Another source of iron catalysts in Fenton reaction could also be the iron powder, which in acid media reacts with hydrogen peroxide producing ferrous ions, Eq. (3) [17]:

$$Fe^0 + H_2O_2 \rightarrow Fe^{2+} + 2OH^- \quad (3)$$

From the environmental point of view, the advantage of the implementation of iron powder (Fe^0) instead of iron salts is that the concentration of iron ions in wastewater after the treatment is significantly lowered [18]. Moreover, utilization of Fe^0/H_2O_2 process takes into account the avoidance of additional loading of treated wastewater with other anions, while a relatively small amount of the remaining iron powder can be easily removed from wastewater after the treatment.

Although UV radiation itself has ability to destroy organic molecules [19], the efficiency of direct photolysis of organic dyes decay proved to be difficult and it depends on the dye's reactivity and photosensitivity [20]. Moreover, most of the commercially used dyes are usually designed to be light resistant. When UV irradiation is combined with some powerful oxidant, such as H_2O_2, organic dye degradation efficiency can be significantly enhanced due to OH radical generation caused by the photolysis of H_2O_2, Eq. (4):

$$H_2O_2 + h\nu \rightarrow 2OH^{\bullet} \quad (4)$$

and these highly reactive non-selective radicals may further react with the organic substrate, i.e. synthetic dye [21]. This process demonstrated high efficiency in the treatment of different types of organic dyes [5,22–24]. UV radiation may also be combined with Fenton or Fenton like processes to improve organic dye decolorization and mineralization in wastewaters [25–30]. Under UV irradiation, Fe^{3+} ions are constantly reduced to the Fe^{2+}, Eq. (5), and the Fenton process is improved by the participation of photogenerated Fe^{2+}:

$$Fe^{3+} + H_2O + h\nu \rightarrow Fe^{2+} + HO^{\bullet} + H^+ \quad (5)$$

The goal of this study was to investigate the efficiency of Fenton type processes, Fe^{2+}/H_2O_2 and Fe^0/H_2O_2, as well as the efficiency of the same processes assisted by UV irradiation, $UV/Fe^{2+}/H_2O_2$ and $UV/Fe^0/H_2O_2$, for the treatment of colored wastewater containing model pollutant, azo dye Acid Orange 7 (AO7). Firstly Fenton type processes were optimized and in the second step combined with UV irradiation to enhance dye degradation. Also, direct photolysis was performed in order to determine a quantum yield of organic dye AO7 by the simple mathematical modeling.

2. Experimental

Azo dye C.I. Acid Orange 7 (AO7), previously synthesized in our laboratory according to the procedure described in the literature [31], was used as the model pollutant (Fig. 1). Experiments were performed using model wastewater with initial dye concentration of 20 mg L^{-1}.

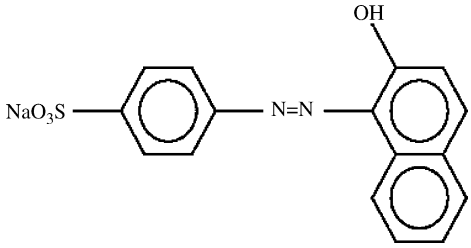

Fig. 1. Structure of C.I. Acid Orange 7.

Series of experiments were conducted in order to establish the optimal iron catalysts/hydrogen peroxide molar ratio for each of the applied Fenton type processes, Fe^{2+}/H_2O_2 and Fe^0/H_2O_2. According to the literature [32–34], at the beginning of the experiment, pH was adjusted at 3 using 25% sulfuric acid, which was followed by the addition of iron catalyst and hydrogen peroxide. Ferrous sulfate, $FeSO_4 \cdot 7H_2O$, and iron powder were used as the sources of iron catalysts in applied Fenton type processes. The concentrations of iron catalysts were 0.5 and 1.0 mM in both processes, while the concentration of hydrogen peroxide was varied to give molar ratios 1:5–50. The reaction mixture ($V = 250$ mL) was continuously stirred at room temperature in the open batch reactor with magnetic stirring bar, and treated for 1 h, while dye concentration and TOC values were measured at the end of each experiment to establish decolorization and mineralization extents.

Experiments with the highest mineralization extents achieved by the usage of Fenton type processes were repeated in the absence and in the presence of UV light radiation. The same photoreactor as in our previous study [35], a water-jacketed glass vessel of total capacity volume of 0.8 L, was used (Fig. 2). A quartz tube was placed vertically in the middle of the photoreactor with mercury lamp 125 W (UV-C, 254 nm) located inside (UVP-Ultra Violet Products, Cambridge, UK, and supplied by Hach Company, Loveland, CO, USA). The UV lamp was attached to a power supply, UVP-Ultra Violet Products, Upland, CA, USA, with the frequency of 50/60 Hz, $U = 230$ V, $I = 0.21$ A. The value of incident photon flux by reactor volume unit at 254 nm, $I_0 = 3.42 \times 10^{-6}$ Einstein L^{-1} s^{-1}, was calculated on the basis of the ferrioxalate actinometry measurements [36]. The total volume of the treated solution was 0.5 mL, while the solution circulated through reactor by a peristaltic pump at a flow rate of 0.1 L min^{-1}. Temperature was maintained at 25 ± 0.2 °C by circulating the water through jacket around the photoreactor. The duration of each experiment was 60 min. Samples were taken periodically from the reactor (0, 2, 5, 10, 20, . . ., 60 min) and thereafter immediately analyzed. All experiments were repeated three times and averages are reported.

A Perkin-Elmer Lambda EZ 201 UV–vis spectrophotometer was used for decolorization monitoring at $\lambda_{max} = 480$ nm, while mineralization extents were determined on the basis of total organic carbon content measurements (TOC), performed by using total organic carbon analyzer; TOC-V_{CPN} 5000 A, Shimadzu. Handylab pH/LF portable pH-meter, Schott Instruments GmbH, Mainz, Germany, was used for pH measurements.

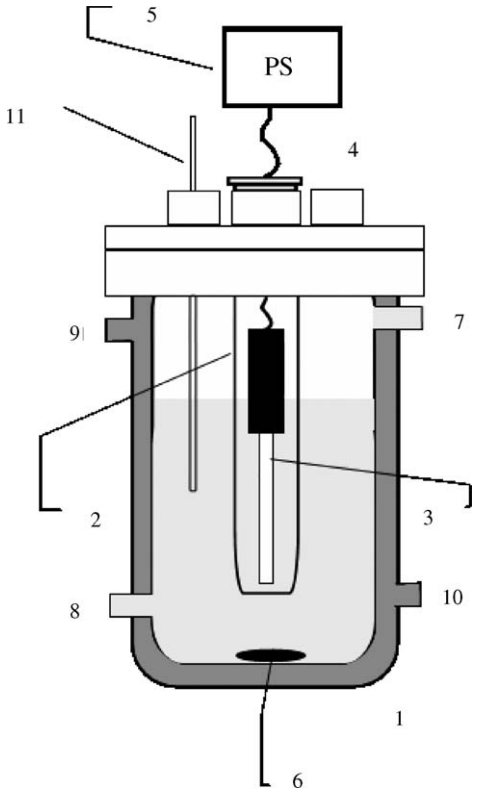

Fig. 2. Schematic diagram of photoreactor: (1) glass water-jacketed reactor, (2) quartz jacket, (3) UV lamp, (4) sampling port, (5) power supply (PS), (6) magnetic stirring bar, (7) and (8) solution inlet and outlet, (9) and (10) cooling water inlet and outlet, (11) thermometer.

3. Results and discussion

According to our previous investigations [37,38] and also the knowledge from the literature [39], the oxidation power of Fenton reagent is influenced by several operating parameters: iron concentration, source of iron catalysts (ferrous or ferric salts, iron powder), H_2O_2 concentration, iron catalyst/hydrogen peroxide ratio, pH, treatment time and temperature. Therefore, it was necessary to find optimal process parameters through the laboratory treatability tests, so-called "jar tests". Thus, in this paper a set of experiments using different sources of iron catalyst and different molar ratios of iron catalyst/H_2O_2 were conducted in order to establish optimal values of studied parameters for both Fenton type processes, Fe^{2+}/H_2O_2 and Fe^0/H_2O_2. Fig. 3 summarizes AO7 decolorization and mineralization results after conducted "jar tests" for determining optimal values of studied parameters for Fe^{2+}/H_2O_2 process. It can be seen that by the usage of both Fe^{2+} concentration, almost complete decolorization of AO7 model solution was obtained. Color removals between 98–99% and 90–95% with iron catalyst concentrations of 0.5 and 1.0 mM were achieved, respectively. Somewhat lower decolorization observed in the cases using higher Fe^{2+} concentration may be attributed to the pronounced interference of dye spectra and spectra of iron complexes. Those complexes are assumed to be formed with possible by-products of dye degradation after the initial cleavage of azo bond. Besides bleaching, degradation of organic dye molecule is characterized by a

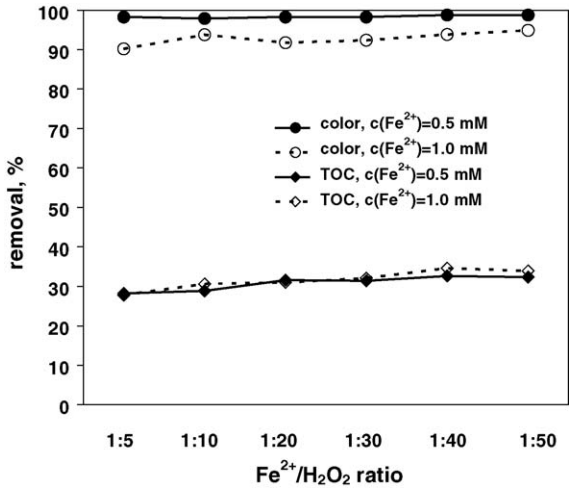

Fig. 3. Influence of ferrous concentration and Fe^{2+}/H_2O_2 ratio on color and TOC removal in Fenton process for the degradation of AO7 at pH 3.

decrease of total organic content, i.e. values of TOC parameter. Almost the same mineralization extents were achieved with both 0.5 and 1.0 mM of ferrous sulfate concentration. It can be seen that with increasing the hydrogen peroxide concentration, degradation efficiency was also slightly increased to the achievement of the certain optimal Fenton reagent ratio. With the further increasing of hydrogen peroxide concentration, degradation efficiency decreased due to the scavenging nature of hydrogen peroxide towards OH radicals when it is present in higher concentration. This resulted in the formation of perhydroxyl radicals which are significantly less reactive than hydroxyl radicals, Eqs. (6) and (7) [17].

$$H_2O_2 + {}^{\bullet}OH \rightarrow HO_2{}^{\bullet} + H_2O \quad (6)$$

$$HO_2{}^{\bullet} + {}^{\bullet}OH \rightarrow H_2O + O_2 \quad (7)$$

The highest mineralization extent, 34.67% of TOC removal, was achieved with $c(Fe^{2+}) = 1.0$ mM and $Fe^{2+}/H_2O_2 = 1{:}40$.

As it was described for "classical" Fenton process, "jar tests" for establishing optimal studied parameters of Fenton like process, Fe^0/H_2O_2, were performed (Fig. 4). In Fe^0/H_2O_2 process, 28 and 56 mg L^{-1} of iron powder were added and they correspond to 0.5 and 1.0 mM iron concentration applied in Fe^{2+}/H_2O_2 process. Again, almost complete bleaching, >98% of color removal was obtained through the entire investigated range of H_2O_2 concentration, but only for a lower dosage of iron powder. On the other hand, with a higher dosage of iron powder, decolorization efficiency strongly depended on Fe^0/H_2O_2 ratio, where constant decreasing in decolorization efficiency by increasing H_2O_2 concentration over 10 mM was observed. The same, but even more pronounced effect can be observed from the results of the partial mineralization of AO7 model solution (Fig. 4). It can be seen that with both used Fe^0 dosages, by increasing H_2O_2 concentration mineralization efficiency also increased to the certain level where with further increasing of H_2O_2 concentration, mineralization efficiency started to sharply decrease. This effect is partially associated with the scavenging nature of H_2O_2 towards OH radicals when it was in excess,

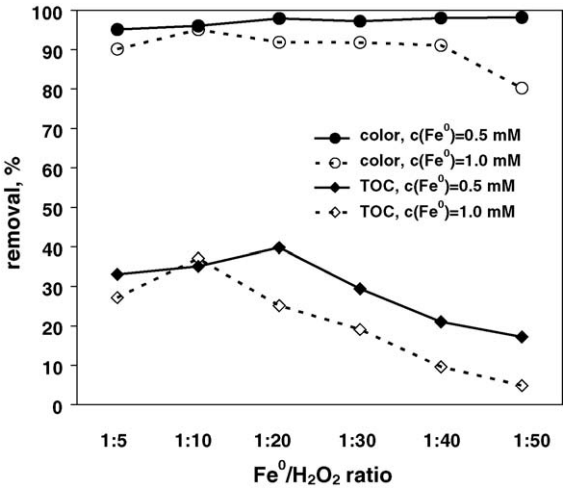

Fig. 4. Influence of iron powder dosage and Fe^0/H_2O_2 ratio on color and TOC removal in Fenton "like" process for the degradation of AO7 at pH 3.

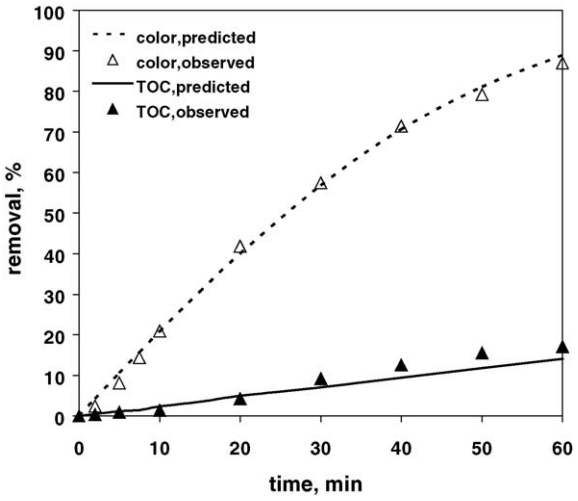

Fig. 5. The efficiency of direct photolysis for the degradation of AO7, the comparison of data predicted by model and those experimentally obtained.

Eqs. (6) and (7). But in the case of iron powder that negative effect of H_2O_2 when it was present in higher concentration, can be mainly attributed to the formation of an inert oxidative film on the iron powder surface which disables further leaching of Fe^{2+} ions in the bulk and continuous generation of OH radical throughout reaction (1) [15]. Again, like in decolorization results, a lower efficiency of Fe^0/H_2O_2 process for the mineralization of AO7 using higher dosage of iron powder was observed. The highest mineralization extent, 39.78% of removed TOC, was obtained in the case of $c(Fe^0) = 0.5$ mM and Fe^0/H_2O_2 ratio of 1:20 (Fig. 4). Maximal mineralization extent obtained by Fe^0/H_2O_2 process was 5.21% higher in comparison to that achieved by Fe^{2+}/H_2O_2, although the concentration of iron catalyst was lower (Figs. 3 and 4). Plausible explanation for that could be found in the fact known from the literature that highly oxidative media promotes oxidation reaction of organic molecules adsorbed on the surface of solid particles [40,41].

Further set of experiments was directed to the investigations of the efficiency of direct UV photolysis for AO7 degradation in model wastewater. The quantum yield of AO7, 6.5×10^{-3} mol Einstein^{-1}, was determined by trial and error method inserting values into the model with simultaneous comparison of predicted and experimentally obtained data for AO7 decolorization. Simulation of AO7 degradation was performed by *Mathematica 5.0* (Wolfram Research, Champaigne, IL) using GEAR method which finds the numerical solution to the ordinary differential equation. The used model, given by Eq. (9), is a modified version of the so-called "LL model", a semiempirical model based on the Lambert's law, proposed in the literature [19]:

$$r_{UV} = -\frac{dc_i}{dt} = \Phi_i F_i I_0[1 - \exp(-2.303L \sum \varepsilon_j c_j)] \quad (8)$$

being $f_i = \varepsilon_i c_i / \sum \varepsilon_j c_j$, where Φ_i, ε_i, I_0 and L stand for the quantum yield and the extinction coefficient of specie i, the incident photon flux by reactor volume unit and the effective optical path in the reactor, respectively. Gimeno et al. [42] proposed that, if only the beginning of the photolysis process was considered, almost all radiation was adsorbed by the parent compound i, and that no other generated intermediates j competed for the absorption of photons. In the latter case, it followed that $\varepsilon_i c_i \approx \varepsilon_j c_j$ and $F_i \approx 1$. Consequently, the Eq. (8) could be modified as:

$$r_{UV} = -\frac{dc_i}{dt} = \Phi_i I_0[1 - \exp(-2.303L\varepsilon_i c_i)] \quad (9)$$

Once I_0, 3.42×10^{-6} Einstein L^{-1} s^{-1} and L, 3 cm, were known by actinometry experiments, the quantum yield of the specie i could be calculated. The value of molar absorption coefficient of AO7, $\varepsilon = 6352.5$ M^{-1} cm^{-1}, was calculated from the Eq. (10) by measuring absorbance of the AO7 solution at 254 nm. Absorbance A, can be expressed as:

$$A = \varepsilon \times l \quad (10)$$

where ε is the molar absorption coefficient with dimensions 1/(concentration × length) and l is the cell path length [43]. From Fig. 5, a good accordance between data for color and TOC removal predicted by used model and data obtained experimentally during the treatment of AO7 model solution by UV photolysis process can be observed. Minor discrepancy between predicted and observed TOC removal in the period after 30 min of treatment, may be attributed to the formation of by-products with different quantum yields which was not included in the modeling. From the decolorization and mineralization point of view, it can be seen that AO7 model solution was partially decolorized up to 87.02%, while only 17.08% of organic content was mineralized. Such behavior of the studied system was expected, due to the fact that commercial synthetic dyes are designed to be light resistant [20]. The very low mineralization extent with only 17.08% of TOC removal, achieved by direct photolysis of AO7 model solution is associated with incomplete decolorization of AO7 model solution. According to Collona et al. [22] decolorization is followed by mineralization, i.e. first the bleaching of the solution to the certain level occurred and afterwards the mineralization process started.

The next step was to establish and to compare the efficiency of Fenton type processes, Fe^{2+}/H_2O_2 and Fe^0/H_2O_2, and the effi-

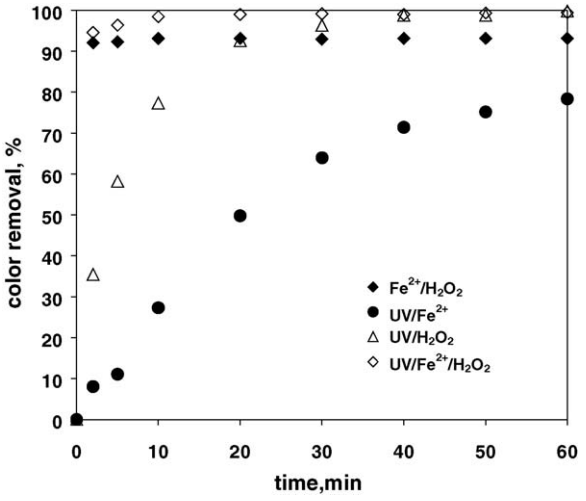

Fig. 6. Color removal of AO7 during the treatments by different AOPs. Initial conditions: $c(Fe^{2+}) = 1.0$ mM, $c(H_2O_2) = 40$ mM, pH 3.

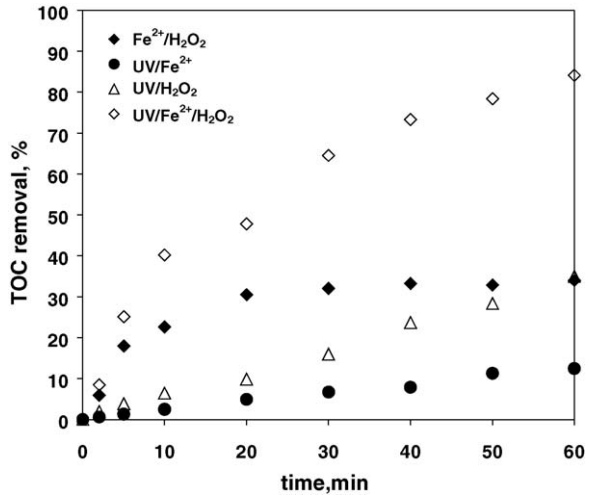

Fig. 7. TOC removal of AO7 during the treatments by different AOPs. Initial conditions: $c(Fe^{2+}) = 1.0$ mM, $c(H_2O_2) = 40$ mM, pH 3.

ciency of the same processes in the presence of UV light, for the decolorization and mineralization of AO7 model solution. The efficiency of corresponding UV/H_2O_2 and UV/iron catalyst processes at optimal conditions of Fenton type processes established earlier (Figs. 3 and 4), were also studied. In Fig. 6, AO7 decolorization kinetics by Fe^{2+}/H_2O_2, UV/Fe^{2+}/H_2O_2, UV/H_2O_2 and UV/Fe^{2+} processes were presented. The concentrations of added ferrous sulfate and hydrogen peroxide were the same as those established as optimal for AO7 degradation by Fenton process in Fig. 3, $c(Fe^{2+}) = 1.0$ mM and $c(H_2O_2) = 40$ mM. AO7 model solution was decolorized up to 93.86% by Fe^{2+}/H_2O_2 process and achieved steady state almost immediately (Fig. 6). As it was mentioned earlier, difference between decolorization achieved and complete decolorization, may be attributed to the interference of dye spectra by the possible formation of Fe-complexes between Fe ions and dye by-products with maximum wavelength close to the λ_{max} of studied dye. In the case of UV/Fe^{2+}/H_2O_2 process more than 95% of color removal was obtained in the second minute, while the complete bleaching, 100% of color removal, was achieved after 20 min of process, leading to the conclusion that UV light is able to destroy formed Fe-complexes. Similar differences of decolorization efficiency between Fe^{2+}/H_2O_2 and corresponding process in the presence of UV light were reported by several authors [29,34]. The complete color removal, 100%, was also achieved by UV/H_2O_2 process due to the OH radical production throughout the H_2O_2 photolysis, reaction (4), but after 40 min of the process. As in the case of direct photolysis, AO7 model solution was decolorized only partially by UV/Fe^{2+} process. Achieved decolorization extent, 78.36%, was even lower than that obtained by direct photolysis of AO7 solution, 87.02% of color removal (Figs. 5 and 6). So, the final achieved decolorization extents followed the increasing order UV/Fe^{2+} < Fe^{2+}/H_2O_2 < UV/H_2O_2 = UV/Fe^{2+}/H_2O_2.

Besides decolorization, process efficiency was estimated on the basis of TOC value decrease (Fig. 7). It can be seen that AO7 model solution was mineralized up to 34.67% with the achievement of steady state after 20 min of Fe^{2+}/H_2O_2 process. Observed inhibition of the mineralization process could be the consequence of either complete consumption of added H_2O_2 or quenching of Fe ions into the stable complexes. According to the AO7 mineralization results during the UV/Fe^{2+}/H_2O_2 process, where continuous degradation of organic content through complete treatment time could be observed, it is more likely that AO7 degradation by Fe^{2+}/H_2O_2 process is inhibited due to the formation of stable Fe-complexes. Thus, the final mineralization extent of 84.12% of TOC removal achieved after 1-h treatment by UV/Fe^{2+}/H_2O_2 process was significantly higher than that by Fe^{2+}/H_2O_2. Kavitha and Palanivelu [44] reported that Fe-complexes can be destroyed under UV irradiation and that iron ions can be returned into the iron regeneration cycle, i.e. formation of OH radicals through Fenton mechanism could be continued. Besides that, in comparison to Fe^{2+}/H_2O_2 process, in UV/Fe^{2+}/H_2O_2 process the generation of OH radicals via photolysis of H_2O_2 and the degradation of organics through direct photolysis additionally attribute to the overall enhancement in mineralization efficiency of AO7. In the case of UV/H_2O_2 process, final mineralization extent achieved after 1-h treatment, 34.99% TOC removal, was almost the same as that obtained by Fe^{2+}/H_2O_2. However, the continuous trend of TOC removal implicates that degradation of remaining organics tends to progress even after 60 min of the treatment, which is not the case in Fe^{2+}/H_2O_2 process. As it was expected due to the incomplete decolorization, the lowest TOC removal (12.45%) was obtained by UV/Fe^{2+} process. The final mineralization extents achieved after 1-h treatment followed the increasing order UV/Fe^{2+} < Fe^{2+}/H_2O_2 = UV/H_2O_2 < UV/Fe^{2+}/H_2O_2.

Fig. 8 presents the calculation of apparent first-order rate constants, k, of the AO7 degradation by above processes for the first 10 min of treatment time by using linear regression, $\ln(TOC/TOC_0)$. It can be seen that the calculated value of k for UV/Fe^{2+}/H_2O_2, 0.0542 min^{-1}, was almost twice as high as k for Fe^{2+}/H_2O_2 process, 0.0285 min^{-1}. These results speak in favor of earlier set forth conclusions which confirm that besides predominant OH radical generation throughout Fenton mechanism, OH radical production via H_2O_2 photolysis significantly attribute to the overall generation of OH radicals. Although sim-

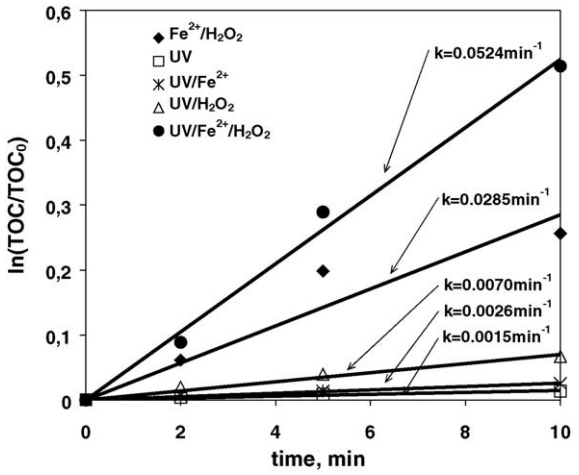

Fig. 8. Comparison of AO7 degradation kinetics during the first 10 min of treatments by different AOPs. Initial conditions: $c(Fe^{2+}) = 1.0$ mM, $c(H_2O_2) = 40$ mM, pH 3.

ilar values of TOC removal were obtained after 1-h treatments by Fe^{2+}/H_2O_2 and UV/H_2O_2 processes, 34.67 and 34.99% TOC removal, respectively, a significantly lower first-order rate constant was calculated for UV/H_2O_2 process, 0.0070 min^{-1}.

Fig. 9 presents the kinetic of AO7 decolorization by Fe^0/H_2O_2, $UV/Fe^0/H_2O_2$, UV/H_2O_2 and UV/Fe^0 processes at 0.5 mM of iron catalyst and/or 10 mM of H_2O_2 which were previously established as optimal for Fe^0/H_2O_2 process (Fig. 4). It can be seen that although decolorization rate of AO7 by Fe^0/H_2O_2 process is somewhat lower than that by Fe^{2+}/H_2O_2 (Fig. 6), final extent is slightly higher, 98.10%. Initial lower rate of AO7 decolorization can be explained by a gradual leaching of Fe^{2+} ions into the solution, reaction (3), and consequently by the slower generation of OH radicals throughout Fenton mechanism [15], reaction (1). On the other hand, the overall higher decolorization extent may be attributed to the lower formation of Fe-complexes due to both lower initial concentration of iron catalyst and gradual leaching of Fe ions from the iron powder surface into the bulk. Complete color removal was obtained by $UV/Fe^0/H_2O_2$ and UV/H_2O_2 processes (Fig. 9) similarly like in the case of processes with the addition of Fe^{2+}-salt and/or H_2O_2 (Fig. 6). Decolorization profile obtained by the treatment with $UV/Fe^0/H_2O_2$ is similar to that obtained by $UV/Fe^{2+}/H_2O_2$ process. It should be emphasized that treatment time required for complete AO7 bleaching in the case of UV/H_2O_2 process with 10 mM of H_2O_2 was 30 min (Fig. 9), while with 40 mM of H_2O_2 it was 40 min (Fig. 6). In the case of UV/Fe^0 process complete decolorization was not achieved, only 84.83% of color was removed, like in cases of AO7 treatment by UV and UV/Fe^{2+} process. Moreover, a slightly lower final decolorization extent was obtained than by UV process, where 87.02% of color was removed (Fig. 5). The plausible explanation for lower extents of decolorization by UV process with the addition of iron catalysts than by direct photolysis of AO7 model solution could be found in the assumption that a part of emitted energy by UV light might be lost to the irradiation of added iron catalysts. The final decolorization efficiency followed the increasing order $UV/Fe^0 < Fe^0/H_2O_2 < UV/H_2O_2 = UV/Fe^0/H_2O_2$ (Fig. 9), similarly like in earlier experiments based on the optimal operating conditions for the Fenton process.

The mineralization efficiency of the processes with the addition of iron powder and/or hydrogen peroxide is compared and presented in Fig. 10. It can be seen that AO7 mineralization by Fe^0/H_2O_2 process was significantly enhanced in the presence of UV irradiation, from 39.78 to 90.09% of removed TOC. As it was mentioned before, achievement of steady states in degradation of organics by Fenton type processes could be the consequence of either complete H_2O_2 consumption or quenching of Fe ions into the stable complexes. In the Fe^0/H_2O_2 process it is more likely that the pronounced inhibition of mineralization rate, which occurred after 20 min of the treatment, might be the result of the complete consumption of added hydrogen peroxide. The results of TOC decrease obtained during the treatment of AO7 model solution by $UV/Fe^0/H_2O_2$ process also state in the favor of this assumption. Moreover, in the same treat-

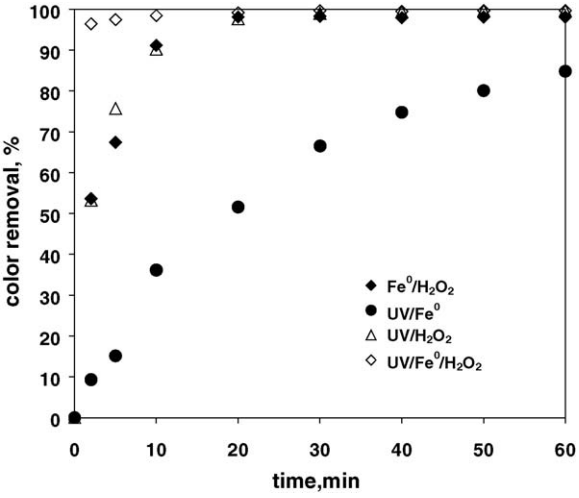

Fig. 9. Color removal of AO7 during the treatments by different AOPs. Initial conditions: $c(Fe^0) = 0.5$ mM, $c(H_2O_2) = 10$ mM, pH 3.

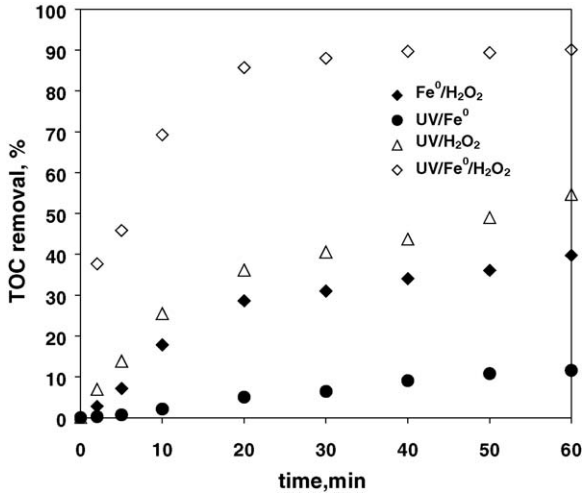

Fig. 10. TOC removal of AO7 during the treatments by different AOPs. Initial conditions: $c(Fe^0) = 0.5$ mM, $c(H_2O_2) = 10$ mM, pH 3.

ment time, after 20 min, even more pronounced reduction in the oxidation power of UV/Fe^0/H_2O_2 process was observed. That was also corroborated by the treatment of AO7 model solution with UV/H_2O_2 process, $c(H_2O_2) = 10$ mM. It can be seen that although after 20 min of the process, mineralization of organics was strongly inhibited, but it was not terminated (Fig. 10). This observation could be explained with the fact that after the consumption of H_2O_2, degradation of organics might be continued through the UV photolysis mechanism and also by chain radical mechanism between organic radicals formed by dye degradation with OH radicals. Chen and Pignatello [45] proposed degradation mechanism of phenol which also includes secondary reactions between organic radicals formed by attack of OH radical to the parent organic molecule, contributing to the overall mineralization extent. Furthermore, Stylidi et al. [3] reported the formation of phenol and other mono-substituted benzenes, di- substituted benzenes, mono- and di-substituted naphtoles and organic acids as by-products of TiO_2 photocatalytic degradation of azo dye Acid Orange 7. Therefore, it can be assumed that the same type of organic radicals which are formed in the phenol degradation could also be formed by OH radical attack to other organics with at least one benzene ring. Similar continuation of mineralization process can be observed by the treatment with Fe^0/H_2O_2 process after 20 min of process (Fig. 10). If there was no UV irradiation, further mineralization could be attributed only to the mentioned chain radical mechanism. As it was expected due to the incomplete decolorization, the lowest mineralization extent, 11.56% of TOC removal, was reached by the treatment with UV/Fe^0 process. Final reached mineralization extents followed the increasing order UV/Fe^0 < Fe^0/H_2O_2 < UV/H_2O_2 < UV/Fe^0/H_2O_2 (Fig. 10). As it was mentioned before, despite lower concentration of iron catalyst, higher mineralization was obtained by Fe^0/H_2O_2 than by Fe^{2+}/H_2O_2 process, 39.78 toward 34.67% of TOC removal (Figs. 7 and 10). Similarly to those results, higher overall mineralization was reached by the same processes in the presence of UV light, UV/Fe^0/H_2O_2 and UV/Fe^{2+}/H_2O_2, 90.09 toward 84.12% TOC removal. Those differences in the efficiency of processes using iron powder and Fe^{2+}-salt could be associated with the earlier mentioned positive effect of solid particles to the highly oxidative media [40,41]. Comparing dye degradation efficiency of both UV/H_2O_2 processes, with 10 and 40 mM of initial hydrogen peroxide concentration, it can be seen that besides shorter time for the achievement of complete decolorization by lower concentration of H_2O_2 (Figs. 6 and 9), a significantly higher mineralization was obtained, 54.66 toward 34.99% TOC removal (Figs. 7 and 10). Reason for that could be found in the fact that at higher concentration in the bulk, hydrogen peroxide is behaving like hydroxyl radical quencher, Eqs. (6) and (7), consequently lowering the hydroxyl radicals concentration, which resulted in lowering the dye degradation efficiency of UV/H_2O_2 process [46].

In Fig. 11 comparison of calculations obtained by linear regression of first-order rate constants for the first 10 min of processes conducted at optimal conditions of Fe^0/H_2O_2 process is presented. It can be seen that the highest k, 0.1225 min^{-1}, was calculated for UV/Fe^0/H_2O_2 process which is more than

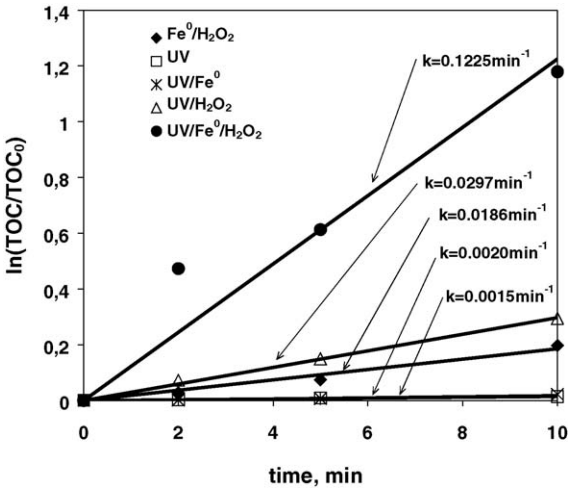

Fig. 11. Comparison of AO7 degradation kinetics during the first 10 min of treatments by different AOPs. Initial conditions: $c(Fe^0) = 0.5$ mM, $c(H_2O_2) = 10$ mM, pH 3.

double high than that calculated for UV/Fe^{2+}/H_2O_2 process, 0.0524 min^{-1} (Fig. 8). The reason could be found in the positive effect of solid particles as well as in significantly higher k for UV/H_2O_2 process with lower H_2O_2 concentration, 0.0297 toward 0.0070 min^{-1} (Fig. 8), which ensured higher additional OH radical production through H_2O_2 photolysis alongside the basic source throughout Fenton mechanism. The proof for the gradual leaching of Fe^{2+} ions from the iron powder surface into the bulk could be found in the lower k for Fe^0/H_2O_2, 0.0186 min^{-1}, than that for Fe^{2+}/H_2O_2, 0.0285 min^{-1}.

From the presented results it could be seen that Fenton type processes using iron powder both in the presence and in the absence of UV light showed higher AO7 degradation efficiency than those using Fe^{2+}-salt. Besides higher efficiency, processes using Fe^0 are more acceptable from the environmental point of view, too. With the usage of iron powder, the loading of treated solution with counter ions is avoided and at the same time concentration of remaining iron ions in the bulk is also lower, even up to 50% [18].

4. Conclusions

Fenton type, Fe^{2+}/H_2O_2 and Fe^0/H_2O_2, and corresponding photo-assisted processes, UV/Fe^{2+}/H_2O_2 and UV/Fe^0/H_2O_2, as well as UV/H_2O_2 processes, were successfully applied for treatment of AO7 model wastewater. Almost complete, >94% bleaching of AO7 solution was achieved by all processes, with exception of direct photolysis and processes combining UV light and iron catalysts, where only partial color removal, <87%, was reached. Significant enhancement of mineralization was achieved in both Fenton type processes in the presence of UV irradiation, from 34.67 up to 84.12% TOC removal for processes using Fe^{2+}-salt and from 39.78 up to the overall highest 90.09% of TOC removal for those using iron powder as iron catalyst. It should be emphasized that besides higher AO7 mineralization efficiency, processes using iron powder are more environmentally friendly because of the lower iron concentrations after

the treatment in the bulk and because of the avoidance of the addition of other anions to the treated system. By using simple mathematical modeling, a quantum yield of studied dye, $\Phi = 6.5 \times 10^{-3}$ mol Einstein^{-1}, was calculated.

Acknowledgements

Financial support from the Ministry of Education, Science and Sport, Republic Croatia, (project # 0125-018) are gratefully acknowledged. We would also like to thank Dr. Ana Loncaric Bozic, Dr. Sanja Papic and Igor Peternel for very useful comments.

References

[1] C. Zhu, L. Wang, L. Kong, X. Yang, L. Wang, S. Zheng, F. Chen, F. MaiZhi, H. Zong, Chemosphere 41 (2000) 303–309.
[2] H. Park, W. Choi, J. Photochem. Photobiol. A: Chem. 159 (2003) 241–247.
[3] M. Stylidi, D.I. Kondarides, X.E. Verykios, Appl. Catal. B: Environ. 40 (2003) 271–286.
[4] R. Nillson, R. Nordlinder, U. Wass, Br. J. Ind. Med. 50 (1993) 65–70.
[5] F.A.P. Costa, E.M. dos Reis, J.C.R. Azevedo, J. Nozaki, Sol. Energy 77 (2004) 29–35.
[6] G.L. Baughman, E.J. Weber, Environ. Sci. Technol. 28 (2) (1994) 267–276.
[7] S. Papic, N. Koprivanac, A. Loncaric Bozic, Color. Technol. 116 (11) (2000) 352–358.
[8] E. Forgacs, T. Cserhati, G. Oros, Environ. Int. 30 (2004) 953–971.
[9] F. Herrera, A. Lopez, G. Mascolo, P. Albers, J. Kiwi, Water Res. 35 (3) (2001) 750–760.
[10] Y.-S. Chen, X.-S. Zhang, Y.-C. Dai, W.-K. Yuan, Sep. Purif. Technol. 34 (1-3) (2004) 5–12.
[11] P.R. Gogate, A.B. Pandit, Adv. Environ. Res. 8 (2004) 501–551.
[12] P.R. Gogate, A.B. Pandit, Adv. Environ. Res. 8 (2004) 553–597.
[13] W.G. Kuo, Water Res. 26 (7) (1992) 881–886.
[14] S.H. Lin, C.C. Lo, Water Res. 31 (1997) 2050–2056.
[15] W.Z. Tang, R.Z. Chen, Chemosphere 32 (5) (1996) 947–958.
[16] M.A. Tarr, in: M.A. Tarr (Ed.), Chemical Degradation Methods for Wastes and Pollutants, Marcel Decker, Inc., New York, 2003, pp. 165–201.
[17] J.A. Bergendahl, T.P. Thies, Water Res. 38 (2004) 327–334.
[18] F. Lücking, H. Köser, M. Jank, A. Ritter, Water Res. 32 (1998) 2607–2614.
[19] F.J. Beltran, in: M.A. Tarr (Ed.), Chemical Degradation Methods for Wastes and Pollutants, Marcel Decker, Inc., New York, 2003, pp. 1–77.
[20] B. Neppolian, H.C. Choi, S. Sakthivel, B. Arabindoo, V. Murugesan, J. Hazard. Mater. B89 (2002) 303–317.
[21] O. Legrini, E. Oliveros, A.M. Braun, Chem. Rev. 93 (1993) 671–698.
[22] G.M. Collona, T. Caronna, B. Marcandalli, Dyes Pigm. 41 (1999) 211–220.
[23] N.H. Ince, Water Res. 33 (4) (1999) 1080–1084.
[24] Y.-S. Shen, D.-K. Wang, J. Hazard. Mater. B89 (2002) 267–277.
[25] F. Ferrero, J. Soc. Dye Colorist 116 (2000) 148–153.
[26] N.H. Ince, G. Tezcanli, Water Sci. Technol. 40 (1) (1999) 183–190.
[27] S.-F. Kang, C.-H. Liao, H.-P. Hung, J. Hazard. Mater. B65 (1999) 317–333.
[28] A. Rathi, H.K. Rajor, R.K. Sharma, J. Hazard. Mater. B102 (2003) 231–241.
[29] M. Neamtu, A. Yediler, I. Siminiceanu, M. Macoveanu, A. Kettrup, Dyes Pigm. 60 (2004) 61–68.
[30] M. Neamtu, A. Yediler, I. Siminiceanu, A. Kettrup, J. Photochem. Photobiol. A: Chem. 161 (2003) 87–93.
[31] K. Venkataraman, The Chemistry of Synthetic Dyes, Academic Press, New York, 1970.
[32] P.K. Malik, S.K. Saha, Sep. Purif. Technol. 31 (3) (2003) 241–250.
[33] S. Meric, D. Kaptan, T. Olmez, Chemosphere 54 (3) (2004) 435–441.
[34] M. Muruganandham, M. Swaminathan, Dyes Pigm. 63 (3) (2004) 315–321.
[35] H. Kušić, N. Koprivanac, A. Lončarić Božić, I. Selanec, J. Hazard. Mater., in press.
[36] H.J. Kuhn, S.E. Braslavsky, R. Schmidt, Pure Appl. Chem. 76 (12) (2004) 2105–2146.
[37] H. Kušić, A. Lončarić Božić, N. Koprivanac, Dyes Pigm. (2005) in press.
[38] S. Papic, N. Koprivanac, A. Loncaric Bozic, D. Vujevic, S. Kucar Dragicevic, H. Kusic, I. Peternel, Water Environ. Res., in press.
[39] www.h2o2.com.
[40] R.D. Vidic, M.T. Suidan, R.C. Brenner, Environ. Sci. Technol. 27 (1993) 2079–2085.
[41] D.R. Grymonpre, W.C. Finney, B.R. Locke, J. Adv. Oxid. Technol. 4 (1999) 408–416.
[42] O. Gimeno, M. Carbajo, F.J. Beltran, F.J. Rivas, J. Hazard. Mater. B119 (2005) 99–108.
[43] P.W. Atkins, Physical Chemistry, fifth ed., Oxford University Press, Oxford, UK, 1994.
[44] V. Kavitha, K. Palanivelu, Chemosphere 55 (2004) 1235–1243.
[45] R. Chen, J.J. Pignatello, Environ. Sci. Technol. 31 (1997) 2399–2406.
[46] M. Muruganandham, M. Swaminathan, Dyes Pigm. 62 (2004) 269–275.